Zinc Titanate Nanopowders. Synthesis and Characterization

M Gabal (mgabalabdonada@yahoo.com)
Chemistry department, Faculty of Science, King Abdulaziz University, Jeddah, KSA
Y.M. Al Angari
Chemistry Department, Faculty of Science, Benha University, Benha, Egypt.

Research Article

Keywords: Zinc titanates, TG, surface are, decomposition, conductivity, dielectric

Posted Date: July 30th, 2021

DOI: https://doi.org/10.21203/rs.3.rs-755010/v1

Version of Record: A version of this preprint was published at Materials Research Express on February 21st, 2022. See the published version at https://doi.org/10.1088/2053-1591/ac5709.

Zinc titanate nanopowders. Synthesis and characterization

M.A. Gabal[a,b,*], Y.M. Al Angari[a]

[a]Chemistry department, Faculty of Science, King Abdulaziz University, Jeddah, KSA

[b]Chemistry Department, Faculty of Science, Benha University, Benha, Egypt.

***Corresponding author.**

E-mail address: mgabalabdonada@yahoo.com

Telephone: 00966557071572

Permanent address: Chemistry Department, Faculty of Science, Benha University, Benha, Egypt.

Abstract:

Zinc titanates nanopowders viz.; Zn_2TiO_4, $ZnTi_3O_8$ and $ZnTiO_3$ were synthesized through the thermal decomposition course of $ZnC_2O_4.2H_2O$-TiO_2 precursor (1:1 mole ratio), prepared via a new co-precipitation method up to 900°C. Thermogravimetric measurement (TG) was utilized to characterize the precursor decomposition while X-ray diffraction (XRD), Fourier transform infra-red (FT-IR) were used to characterize the decomposition products as well as the phase transitions at different temperatures. XRD revealed the starting of titanates formation at 700°C via detecting Zn_2TiO_4 along with ZnO and TiO_2 (anatase) diffraction peaks. By increasing the calcination temperature to 800°C, the ZnO content vanished with the appearing of $Zn_2Ti_3O_8$ besides $ZnTi_2O_4$ and impurities of TiO_2 (anatase). Finally at 900°C, the $Zn_2Ti_3O_8$ content was decomposed into $ZnTiO_3$. Nitrogen adsorption-desorption isotherm of the calcined precursor at 900°C indicated low specific surface area of 7.1 $m^2\ g^{-1}$ in accordance with the agglomeration nature estimated via transmission electron microscopy (TEM) study. The conductivity measurements showed semiconducting behavior of the prepared titanates with ferroelectric transition in the range 200-308°C.The obtained low dielectric value suggests the uses of present titanates as a co-fired ceramic or resonator ceramics.

Keywords: Zinc titanates; TG; surface are; decomposition; conductivity; dielectric.

1. Introduction

Perovskite oxides; $MTiO_3$ titanates (M = Zn, Sr, Fe, Cd, Ba, Pb, etc.) have been regarded as materials having various applications in solid-oxide fuel cells electrodes; SOFCs [1], metal–barriers [2], sensors [3], electronics [4] and catalysts [5]. As a well-known member of this family, Zinc titanate ($ZnTiO_3$) was already used as pigment [6], dye adsorbent [7], sensor for NO and CO gases [8], microwave resonator materials [9], heat reflective pigment [10] and photocatalyst [11].

Based on the literature [6,12,13], there are three phases existing in the system of ZnO-TiO_2: zinc orthotitanate; Zn_2TiO_4 having cubic spinel structure, $Zn_2Ti_3O_8$ having defect cubic structure and metatitanate; $ZnTiO_3$ with ilmenite rhombohedral structure. Zn_2TiO_4 could be easily prepared using conventional ceramic technique using 2:1 mole ratio of ZnO:TiO_2 and is considered to be stable up to 1418^{o}C. On the other hand, metastable $Zn_2Ti_3O_8$ is considered as the low temperature form of $ZnTiO_3$ up to 820^{o}C. Finally, the ilmenite form; $ZnTiO_3$ is very hard to obtain since it decomposes into orthotitanates; Zn_2TiO_4 and TiO_2 (rutile) at 945^{o}C.

The different preparation methods for all zinc titanate phases are reviewed [6]. Co-precipitation method can be considered as the most successful one for obtaining ultrafine powder with narrow size distribution. Using this method, the more complex steps could be avoided besides less time consumption and high purity compared to other methods.

In the present manuscript, a simple coprecipitation technique will be followed to synthesize nano-crystalline zinc titanate powders. In this technique, a stoichiometric co-precipitated mixture of $ZnC_2O_4.2H_2O$-TiO_2 (1:1 mole ratio) will be thermally decomposed up to the titanate formation. To our best knowledge, this is the first report on the synthesis of zinc titanate nanopowder by this method in the literature. The titanate phase's formation as well as their structure characterization, morphology and phase transitions will be investigated via TG-

DTG, XRD, FT-IR, TEM and BET measurements. The different electrical properties viz. ac-conductivity as well as dielectric property will also be evaluated.

2. Experimental procedures

2.a. Materials

Basic zinc carbonate monohydrate; $ZnCO_3.2Zn(OH)_2.H_2O$, unhydrous oxalic acid; $H_2C_2O_4$ and titanium dioxide (anatase); TiO_2 all are of analytical grade (BDH) and utilized as received.

2.b. Synthesis process

The entire titanates were prepared in the present study via the thermal decomposition of oxalate-titania precursor; $ZnC_2O_4.2H_2O$-TiO_2 (1:1 mole ratio). A new innovative route for the preparation of this precursor was utilized in which, a stoichiometric amount of oxalic acid solution equivalent to precipitate zinc oxalate was added drop wisely to the calculated amount of basic zinc carbonate and titania suspension under vigorous stirring at about 60^{o}C. after complete precipitation, the zinc oxalate is expected to precipitate on TiO2 surface through heterogeneous nucleation [14]. The prepared precursor was filtered, washed with distilled water, dried then given the name; as-prepared precursor. To characterize the precursor decomposition route until titanate formation, different samples were calcined in a muffle furnace at 400^{o}C for 30 min, 500 and 600^{o}C for 1h and for 2h at 700, 800 and 900^{o}C.

2.c. Characterization

Thermogravimetric analysis (TG) of the prepared precursor was conducted in air by a Perkin Elmer thermal analyzer (STA 6000) at heating rate of 5^{o}C/min up to 1100^{o}C. The crystal phases were estimated by X-ray diffraction (Bruker AXS) with Cu Kα radiation (λ =

1.5418 Å). The titanates sample were morphologically characterized using transmission electron micrograph (JEOL-2010) with 100 kV accelerating voltage. FT-IR spectra were measured using a JASCO FT-IR 310 spectrophotometer. Specific surface area was measured using BET adsorption and ASAP 2010 analyzer. In electrical measurements, the calcined powders were pressed into pellets (1 cm diameter and 1mm thickness) using 2 ton.cm^{-2} pressure. The two probe method was then used for measuring the temperature dependence of conductivity and dielectric constant at different frequencies (1-1000 kHz), using a Hioki LCR bridge model 3531.

3. Results and discussion

3.a. Thermal decomposition of $ZnC_2O_4.2H_2O$-TiO_2 precursor

The full decomposition course of $ZnC_2O_4.2H_2O$-TiO_2 precursor (Fig. 1), up to 1000^{o}C in air, consists of three well-defined TG steps. According to the calculated weight losses, the first two steps could be attributed to the loss of water with the formation of anhydrous ZnC_2O_4-TiO_2 mixture. The calculated weight loss (14.0 %) for the dehydration process agreed well with that experimentally obtained (13.9 %) up to about 240^{o}C. The dehydration process was found to occur through two separated TG steps in the temperature ranges; 100-125 and 215-240^{o}C, respectively which are characterized by two differential thermogravimetric (DTG) peaks at 116 and 226^{o}C. According to Diefallah [15], the water lost at low temperature range can be considered as crystal water while that lost at higher temperatures as coordinately bounded.

In the third TG step appeared in the range from 306 to 387^{o}C (with DTG peak at 362^{o}C), the observed weight loss (25.5 %) agreed well with the calculated one of 26.5 % attributed to the decomposition of the oxalate content with the formation of ZnO-TiO_2 mixture and evolution of Co and CO_2 as decomposition products [16]. No further weight changes could be observed up to 1000^{o}C.

3.b. X-ray diffraction and titanates formation

The thermal decomposition course of the studied precursor as well as the titanates formation was successfully followed using XRD measurements of calcined precursor samples at temperatures ranging between 400 and 900°C. Fig. 2 illustrates XRD patterns of the different calcined samples along with the different phases formed during calcination process. XRD pattern of the as-prepared precursor indicated the characteristic individual diffraction peaks of both monoclinic $ZnC_2O_4.2H_2O$ and tetragonal TiO_2 (anatase) according to the JCPDS file Nos. (25-1029) and (78-2486), respectively. This confirmed well the complete reaction between basic zinc carbonate and oxalic acid without any indication for the presence of any side products.

XRD pattern of the sample calcined at 400°C showed, in agreement with the decomposition course (Fig. 1), the presence of hexagonal ZnO and tetragonal TiO_2 (anatase). The obtained diffraction peaks agree well with those presented in the JCPDS file Nos. (79-0206) and (78-2486), respectively. The no indication for the presence of any peaks characteristic for titanates at this calcination temperature confirmed the inability of any interaction between the decomposition products. The only observed change in the diffraction patterns for samples calcined at 500 and 600°C (Fig. 2) is the obvious improvement in the samples crystallinity without the indication for the appearing of any new phase.

For the sample calcined at 700°C, the obvious appearance of new XRD peaks characteristic for face-centered cubic Zn_2TiO_4 (JCPDS file No. 73-0578) besides the still exist of ZnO and TiO_2 (anatase) peaks indicated the just initiation of the interaction between mixed oxides and titanates formation. In literature, lot of investigations [17-19] were reported on the inability of pure $ZnTiO_3$ formation from 1:1 mole ratios of ZnO and TiO_2 mixture. Others [20-22] succeeded to prepare pure $ZnTiO_3$ phase using sol-gel methods. On the other hand, many researchers [19, 23-26] obtained a mixture of titanates such as $ZnTiO_3$, $Zn_2Ti_3O_8$ and Zn_2TiO_4

with Zn_2TiO_4 as major phase. Ivanova et al. [27] and Yan et al. [28] prepared Zn_2TiO_4, TiO_2 and ZnO via sol-gel and hydrothermal routes, respectively using 1:1 mole ratio of Zn:Ti mixture. Siriwong and Phanichphant [29] prepared Zn_2TiO_4 single-phase using 1: 1 mole ratio of zinc naphthenate and titanium tetra isopropoxide precursors by the flame spray pyrolysis technique.

The precursor calcined at 800°C showed the complete vanishing of ZnO diffraction peaks with the appearance of diffraction peaks characteristic for the presence of Zn_2TiO_4 and $Zn_2Ti_3O_8$ (JCPDS file No. 87-1781) phases indicating the complete titanates formation. The $Zn_2Ti_3O_8$ with a defect cubic spinel structure, was first discovered by Yamaguchi et al. [17] and is considered as the low temperature phase of $ZnTiO_3$. The presence of very weak peaks attributed to the presence of TiO_2 (anatase) could be ascribed to the reduction of very few amount of ZnO to volatile elemental Zn [21].

Liu et al. [26] reported that the formation of Zn_2TiO_4 and $Zn_2Ti_3O_8$ phases could only happen in the presence of anatase whereas $ZnTiO_3$ formation is limited only in the presence of rutile. They also reported that, when anatase grains are small enough then, it could be completely utilized in the formation of Zn_2TiO_4 and $Zn_2Ti_3O_8$ while if they are large enough, an anatase to rutile transition would be took place with increasing probability for $ZnTiO_3$ formation. In this context, the estimated grain size of the anatase phase (for the sample calcined at 700°C) using the strongest peak (101) and Scherrer`s equation [30] amounts to 67 nm which is expected to be small enough to form Zn_2TiO_4 and $Zn_2Ti_3O_8$ mixture.

The calculated grain size of the very few amount of anatase in the sample calcined at 800°C (using the strongest peak 101) is about 104 nm which is large enough for anatase-rutile transition and $ZnTiO_3$ formation. This why the XRD pattern of the sample calcined at 900°C indicated the presence of hexagonal $ZnTiO_3$ (JCPDS file No. 25-0671). The decomposition of metastable $Zn_2Ti_3O_8$ into $ZnTiO_3$ and TiO_2 (anatase) by increasing calcination temperature to

900ºC illustrates the increasing amount of $ZnTiO_3$. Again, the presence of weak diffraction peaks characteristic of rutile phase (JCPDS file No. 21-1276) confirmed the anatase-rutile transition and $ZnTiO_3$ formation.

Really, the reason for selecting the (1:1) mole ratio of ZnC_2O_4:TiO_2 in the present preparation was that this ratio would correspond to the stoichiometric $ZnTiO_3$. Instead, the above XRD study indicated the formation of different zinc titanate phases including: $ZnTiO_3$, Zn_2TiO_4 and $Zn_2Ti_3O_8$. Accordingly, the phase transitions along the present decomposition could be represented as:

$$ZnC_2O_4.2H_2O\text{-}TiO_2 \rightarrow ZnC_2O_4\text{-}TiO_2 \rightarrow ZnO\text{-}TiO_2 \rightarrow ZnO + \text{anatase} + Zn_2TiO_4 \rightarrow$$

$$Zn_2TiO_4 + Zn_2Ti_3O_8 + \text{anatase} \rightarrow Zn_2TiO_4 + Zn_2Ti_3O_8 + \text{anatase} + \text{rutile}$$

3.c. FT-IR spectroscopic study

The thermal decomposition course of the entire precursor as well as the titanates formation was also characterized using FT-IR spectroscopy. The characteristic bands obtained for the as-prepared precursor and samples calcined at different temperatures are exhibited in Fig. 3. The precursor sample showed a very broad FT-IR bands around 3441 and 1652 cm^{-1} assigned to the stretching vibration of O-H bond of water in hydrated zinc oxalate molecule. The vibration band at about 1302 cm^{-1} could be attributed to the symmetric mode of oxalate ion`s carbonyl group [14]. The observed bands at 773 and 506 cm^{-1} are attributed to the out-of-plane and in-plane bending modes of water and O–C–O of oxalate, respectively while the band at 348 cm^{-1} could be assigned to the metal ion vibration [31]. Finally, the bands at 680 and 2924 cm^{-1} are attributed to TiO_2 [32].

The calcined precursor at 400°C showed a decrease in the band intensities due to the carbonyl group as a result of oxalate content`s decomposition with the formation of metal oxides as discussed above in TG and XRD results. Thus, the broad band appeared at 525 cm^{-1}

can be assigned to the metal-oxygen (M-O). The further appearance of the bands characteristic of water at 3441 and 1652 cm^{-1} could be attributed to the presence of adsorbed water formed during sample preparation. The samples calcined at 500 and 600°C indicated nearly the same bands indicated same composition without any chance for titanate formation.

The calcined samples at 700, 800 and 900°C indicated alike patterns with an apparent absorption band at 583 cm^{-1} ascribed to Ti–O stretching vibration due to [TiO_6] octahedron group existing in all titanates forms of Zn_2TiO_4, $Zn_2Ti_3O_8$ and $ZnTiO_3$ as previously reported [20,21].

3.d. Morphological study

XRD pattern of the sample calcined at 900°C (Fig. 2), as previously described, indicated two types of particles including Zn_2TiO_4 and $ZnTiO_3$ besides traces of TiO_2. In agreement with this result, TEM image of the calcined precursor at 900°C (Fig. 4) exhibited two distinct types of particles having different sizes. Generally, the particles are nearly spherical with particle sizes of about 60 and 130 nm and exhibited a dense aggregation. A similar result was obtained by Arin et al. [33] for zinc titanates synthesized via hydrothermal method.

3.e. Surface area characterization

Nitrogen adsorption-desorption isotherm of the calcined precursor at 900°C (Fig. 5) exhibited, according to the IUPAC classification [34], type II isotherm in which the adsorption is on macroporous adsorbents through strong adsorbate-adsorbent interaction. This type exhibited also a very small hysteresis as appeared in Fig. 5. The specific surface area (SSA) calculated according to BET method is about 7.1 $m^2\ g^{-1}$ which can be considered as the surface area of Zn_2TiO_4 and $ZnTiO_3$ main contents. This very low surface area could be attributed in accordance with the TEM image (Fig. 4) to the agglomeration nature of the powder which

lowering porosity. Pore size distributions (BJH) (inset of Fig. 5) showed narrow distribution characterized by three pore size types located around 19, 28 and 42 nm.

3.f. Electrical properties measurements

3.f.i. ac-conductivity

The ac-conductivity measured at different applied frequencies by changing temperature from 30 to 450ºC have been studied. The $\ln\sigma$ vs. 1000/*T* plot at frequencies ranging between 1 kHz and 1 MHz for the sample calcined at 900ºC is shown in Fig. 6(a). The conductivity showed a decreasing behavior by increasing temperature up to about 90ºC. During sample`s preparation for conductivity measurements, some water molecules were adsorbed on the titanates surface. This water can be acting as conductor and its removal by increasing temperature could result in decreasing conductivity. Similar behavior was already reported in literature during conductivity measurements [35].

The conductivity showed frequency dependence at low temperatures, in which conductivity increases with increasing frequency, while it indicated frequency independence at higher temperatures. This behavior could be described based on the pumping force of the applied frequency which facilitate the charge carriers' transfer. By increasing temperature, the generated phonons resist the moving of the charge carriers through phonon-electron collisions and thus canceling the applied frequency effect [36].

The estimated conductivity at 110ºC (i.e. temperature at complete adsorbed water evaporation) and frequency of 1 MHz amounts to 6.4×10^{-7} ohm^{-1} cm^{-1}. The conductivity is appeared to be temperature dependent after 110ºC and showed a gradual increase with increasing temperature which reflects semiconducting behavior of the present studied titanates. An anomalous behavior was observed in the rising portion of the curve by increasing temperature in the range 200-308ºC. By a closer look to Fig. 6(a), this anomalous behavior,

appeared as a transition peak, is clearer at higher frequencies (≥ 500 kHz) and also indicated a gradual change in the peak position to lower temperature by increasing frequency.

Chang et al. [37] reported an anomalous strong decrease (exponential decrease) in conductivity vs. reciprocal temperature close to the ferroelectric Curie temperature (T_C) in most perovskite type structure such as $ZnTiO_3$. Such anomalous behavior is well-known as positive temperature coefficient of resistivity (PTCR) [38] and was attributed to electrical potential barrier resulted from the existence of a two-dimensional surface layer of acceptor ions or oxygen adsorbed at grain boundaries [39]. The increase in the applied frequency is expected to decrease the electrical potential barrier and thus shifts the Curie temperature towards lower temperature.

The conduction activation energies (E_a), in the high temperature range using Arrhenius equation: $\sigma = \sigma_0 \exp^{-(E_a / KT)}$, were calculated as a function of frequencies, using $\ln\sigma$ vs 1000/T plot (Fig. 6(a)), and summarized in Table 1. The estimated values agree well with the obtained semiconducting behavior and suggested that the conduction is through the electron hopping [36]. The reported values showed a gradual decrease with increasing frequency, agreed well with the obvious increase in conductivity, attributed to the effect of applied frequency in facilitating charge carriers transfer.

It is well known that, ac conductivity depends on the capacitance and thus on the material`s dielectric property. This behavior may be assigned to the space charge polarization present in the material [40]. Consequently, the observed anomalous observed in the dielectric constant ($\varepsilon`$) vs. temperature relation at different applied frequencies (Fig. 6 (b)), agrees well with that obtained in the conductivity temperature relation (Fi6. 6(a)). At this observed transition, the electric dipoles are disorderly arranged due to the asymmetric shift in the crystal axis`s symmetry with respect to the effective polarization direction. As a result, an abrupt increase in the value of dielectric constant is observed [41,42].

The room temperature dielectric value obtained at applied frequency of 1MHz (Fig. 6(b)) is 43 which is higher than that reported for $ZnTiO_3$ prepared by chemical deposition of 25 [43] and solid-state conventional method of 30 [23]. This obtained dielectric value suggests the uses of present titanates as a co-fired ceramic or resonator ceramics [43].

4. Conclusions

$ZnC_2O_4.2H_2O$-TiO_2 precursor (1:1 mole ratio), synthesized via a new co-precipitation method, was successfully utilized for the preparation of zinc titanate nanopowders. The thermal decomposition of this precursor was resulted in the formation of a mixture of Zn_2TiO_4, $ZnTi_3O_8$ and $ZnTiO_3$ titanates in nanocrystalline form along with very tiny amount of both forms of TiO_2 (anatase and rutile). The present decomposition course has not been reported previously in literature and the different phases formed along the decomposition at different temperatures were characterized using TG, XRD, FT-IR and TEM to estimate the different phase's transitions. The titanates formation started at about 700^{o}C with the formation of Zn_2TiO_4 along with secondary phases of ZnO and TiO_2 (anatase). At 800^{o}C, $Zn_2Ti_3O_8$ started to appear, besides $ZnTi_2O_4$ and impurities of TiO_2 (anatase), and at 900^{o}C it showed its decomposition into $ZnTiO_3$. The conductivity measurements showed semiconducting behavior and indicated ferroelectric transition in the range 200-308^{o}C.The obtained dielectric value suggests the uses of present titanates as a co-fired ceramic or resonator ceramics.

Acknowledgement

This project was funded by the Deanship of Scientific Research (DSR) at King Abdulaziz University, Jeddah, under grant no. (G: 680-130-1441). The authors, therefore, acknowledge with thanks DSR for technical and financial support.

References

[1] B. H. Smith, W. C. Holler, M. D. Gross, Electrical properties and redox stability of tantalum-doped strontium titanate for SOFC anodes, Sol. State Ion. 192 (2011) 383-386.

[2] Y. Liu, L. Li, J. Shi, R. Han, P. Wu, X. Yue, Z. Zhou, G. Chen, Q. Li, High dielectric constant composites controlled by a strontium titanate barrier layer on carbon nanotubes towards embedded passive devices, Chem. Eng. J. 373 (2019) 642-650.

[3] X. Fang, O. K. Tan, Y. Y. Gan, M. S. Tse, Novel immunosensor platform based on inorganic barium strontium titanate film for human IgG detection, Sens. Act. B 149 (2010) 381-388.

[4] H.L. Chan, S.H. Choy, C.P. Chong, H.L. Li, P.C. Liu, Bismuth sodium titanate based lead-free ultrasonic transducer for microelectronics wirebonding applications, Ceram. Int. 34 (2008) 773-777.

[5] F. Liu, H. He, C. Zhang, Z. Feng, L. Zheng, Y. Xie, T. Hu, Selective catalytic reduction of NO with NH_3 over iron titanate catalyst: Catalytic performance and characterization, App. Cat. B 96 (2010) 408-420.

[6] M.R. Mohammadi, D.J. Fray, Low temperature nanostructured zinc titanate by an aqueous particulate sol-gel route: Optimisation of heat treatment condition based on Zn:Ti molar ratio, J. Eur. Ceram. Soc. 30 (2010) 947–961.

[7] R.S. Raveendra, P.A. Prashanth, R.H. Krishna, N.P. Bhagya, B.M. Nagabhushana, H.R. Naik, K. Lingaraju, H. Nagabhushan, B.D. Prasad, Synthesis, structural characterization of nano $ZnTiO_3$ ceramic: An effective azo dye adsorbent and antibacterial agent, J. Asian Ceram. Soc. 2 (2014) 357–365.

[8] C. Lin, J. Chen, W. Feng, C. Lin, J. Huang, J. J. Tunney, K. Ho, Using a TiO_2/ZnO double-layer film for improving the sensing performance of ZnO based NO gas sensor, Sens. Act. B 157 (2011) 361-367.

[9] I. Golovina, I. Geifman, A. Belous, New ceramic EPR resonators with high dielectric permittivity, J. Magn. Resonance 195 (2008) 52-59.

[10] J. Lva, M. Tang, R. Quan, Z. Chai, Synthesis of solar heat-reflective $ZnTiO_3$ pigments with novel roof cooling effect, Ceram. Int. 45 (2019) 15768–15771.

[11] R. Abirami, C.R. Kalaiselvi, L. Kungumadevi , T.S. Senthil, M. Kang, Synthesis and characterization of $ZnTiO_3$ and Ag doped $ZnTiO_3$ perovskite nanoparticles and their enhanced photocatalytic and antibacterial activity, J. Sol. State Chem. 281 (2020) 121019.

[12] Y. Chang, Y. Chang, I. Chen, G. Chen, Y. Chai, S. Wu, T. Fang, The structure and properties of zinc titanate doped with strontium, J. alloys Compd. 354 (2003) 303–309.

[13] J. Luo, X. Xing, R. Yu, Q. Xing, D. Zhang, X. Chen, Synthesis and characterization of $(Zn,Co)TiO_3$ by modified low temperature preparing route, J. alloys Compd.402 (2005) 263–268.

[14] M.A. Gabal, Synthesis and Characterization of Nanocrystalline $PbTiO_3$, Ind. Eng. Chem. Res. 50 (2011) 13771-13777.

[15] El-H.M. Diefalla, Kinetic analysis of thermal decomposition reactions: Part VI. Thermal decomposition of manganese (II) acetate tetrahydrate, Thermochim. Acta 202 (1992)1-16.

[16] D. Dollimore, D.L. Griffiths, Differential thermal analysis study of various oxalates in oxygen and nitrogen, J. Therm. Anal. 2 (1970) 229-250.

[17] O. Yamaguchi, M. Morimi, H. Kawabata, K. Shimizu, Formation and transformation of $ZnTiO_3$, J. Am. Ceram. Soc., 70 (1987) C97–C98.

[18] H.T. Kim, Y. Kim, M. Valant, D. Suvorov, Titanium Incorporation in Zn_2TiO_4 Spinel Ceramics, J. Amer. Ceram. Soc. 84 (2001) 1081–1086.

[19] Z. Cai, J. Li, Y. Wang, Fabrication of zinc titanate nanofibers by electrospinning technique, J. Alloys Compd. 489 (2010) 167–169.

[20] L. Hou, Y. Hou, M. Zhu, J. Tang, J. Liu, H. Wang, H. Yan, Formation and transformation of $ZnTiO_3$ prepared by sol–gel process, Mater. Lett. 59 (2005) 197– 200.

[21] Y. Yu, M. Xia, Preparation and characterization of $ZnTiO_3$ powders by sol–gel process, Mater. Lett. 77 (2012) 10–12.

[22] L. Wang, H. Kang, D. Xue, C. Liu, Low-temperature synthesis of $ZnTiO_3$ nanopowders, J. Cryst. Growth 311 (2009) 611-614.

[23] A. Chaouchi, M. Aliouat, S. Marinel, S. d'Astorg, H. Bourahla, Effects of additives on the sintering temperature and dielectric properties of $ZnTiO_3$ based ceramic, Ceram. Int. 33 (2007) 245–248.

[24] M.V. Nikolic, N. Labus, M.M. Ristic, Densification rate and phase structure changes during sintering of zinc titanate ceramics, Ceram. Int. 35 (2009) 3217–3220.

[25] S.K. Manika, S.K. Pradhan, Preparation of nanocrystalline microwave dielectric Zn_2TiO_4 and $ZnTiO_3$ mixture and X-ray microstructure characterization by Rietveld method, Physica E 33 (2006) 69–76.

[26] Z. Liu, D. Zhou, S. Gong, H. Li, Studies on a basic question of zinc titanates, J. Alloys Compd. 475 (2009) 840–845.

[27] T. Ivanova, A. Harizanova, T. Koutzarova, B. Vertruyen, Preparation and characterization of ZnO–TiO_2 films obtained by sol-gel method, Journal of Non-Crystalline Solids 357 (2011) 2840–2845.

[28] X. Yan, C. Zhao, Y, Zhou, Z. Wu, J. Yuan, W. Li, Synthesis and characterization of $ZnTiO_3$ with high photocatalytic activity, Trans. Nonferrous Met. Soc. China 25 (2015) 2272-2278.

[29] C. Siriwong, S. Phanichphant, Flame-made single phase Zn_2TiO_4 nanoparticles, Mater. Lett. 65 (2011) 2007–2009.

[30] B.D. Cullity, Elements of X-ray Diffraction, 2nd ed. Addison-Wesley, Reading, MA; (1978).

[31] J.M. Ouyang, H. Zheng, S.P. Deng, Simultaneous formation of calcium oxalate (mono-, di-, and trihydrate) induced by potassium tartrate in gelatinous system, J. Cryst. Growth 293 (2006) 118.

[32] R.A. Nyquist, R.O. Kagel, The handbook of infrared and Raman spectra of inorganic compounds and organic salts. Academic Press, San Diego (1997).

[33] J. Arin, S. Thongtem, A. Phuruangrat, T. Thongtem, Characterization of ZnO–TiO_2 and zinc titanate nanoparticles synthesized by hydrothermal process, Res. Chem. Intermed. 43 (2017) 3183–3195.

[34] K.S.W. Sing, D.H. Everett, R.A.W. Haul, L. Moscou, R.A. Pierotti, J. Rouquerol, T. Siemieniewska, Reporting physisorption data for gas/solid systems with special reference to the determination of surface area and porosity, Pure Appl. Chem. 57 (1985) 603-619.

[35] M. A. Gabal, A. A. Al-Juaid, Structural and electromagnetic studies of $Mg_{1-x}Zn_xFe_2O_4$ nanoparticles synthesized via a sucrose autocombustion route, J. Mater. Sci.: Mater. Electr. 31 (2020) 10055–10071.

[36] M.A. Gabal, S.A. Hameed, A.Y. Obaid, $CoTiO_3$ via cobalt oxalate–TiO_2 precursor. Synthesis and characterization, Mater. Charact. 71 (2012) 87–94.

[37] Y. Chang , Y. Chang, I. Chen, G. Chen, Y. Chai, T. Fang, S. Wu, Synthesis, formation and characterization of $ZnTiO_3$ ceramics, Ceram. Int. 30 (2004) 2183–2189.

[38] J. Daniels, K.H. Härdtl, R. Wernicke, The PTC effect of barium titanate, Philips Tech. Rev. 38 (3) (1978) 73–82.

[39] W. Heywang, Resistivity anomaly in doped barium titanate, J. Am. Ceram. Soc. 47 (1964) 484–490.

[40] N.K. Singh, P. Kumar, R. Rai, J. Alloys Compd. Study of structural, dielectric and electrical behavior of $(1-x)Ba(Fe_{0.5}Nb_{0.5})O_3-xSrTiO_3$ ceramics, 509 (2011) 2957.

[41] M. Chakraborty, S. Chaudhuri, V.K. Rai, V. Mishra, Investigation on the electrical and optical properties of some zinc titanate ceramics, J. Mater. Sci.: Mater. Electron. Pramana – J. Phys. 92 (2019) 46.

[42] Z. Gao, C. Lu, Y. Wang, S. Yang, Y. Yu, H. He, Super Stable Ferroelectrics with High Curie Point, Sci. Rep. 6 (2016) 24139.

[43] I. Bobowska, A. Opasinska, A. Wypych, P. Wojciechowski, Synthesis and dielectric investigations of $ZnTiO_3$ obtained by a soft chemistry route, Mater. Chem. Phys. 134 (2012) 87– 92.

Figure captions

Fig. 1: TG-DTG curves for the thermal decomposition of $ZnC_2O_4.2H_2O$-TiO_2 (1:1) precursor in air. Heating rate = 5ºC min^{-1}.

Fig. 2. XRD patterns of $ZnC_2O_4.2H_2O$-TiO_2 (1:1) precursor calcined at different temperatures.

Fig. 3. FT-IR spectra of $ZnC_2O_4.2H_2O$-TiO_2 (1:1) precursor calcined at different temperatures.

Fig. 4. TEM image of calcined precursor at 900ºC for 2h. Scale bar, 100 nm.

Fig. 5. N_2 adsorption/desorption isotherm obtained for calcined precursor at 900ºC for 2h.

Fig. 6. Electrical properties of calcined precursor at 900ºC for 2h. (a) $\ln\sigma$ vs. $1000/T$ as a function of applied frequency. (b) Dielectric constant vs. absolute temperature as a function of applied frequency.

Table caption

Table 1. Activation energies calculated from ln σ vs. 1000/T plot as a function of frequencies for calcined precursor at 900ºC for 2h

Figures

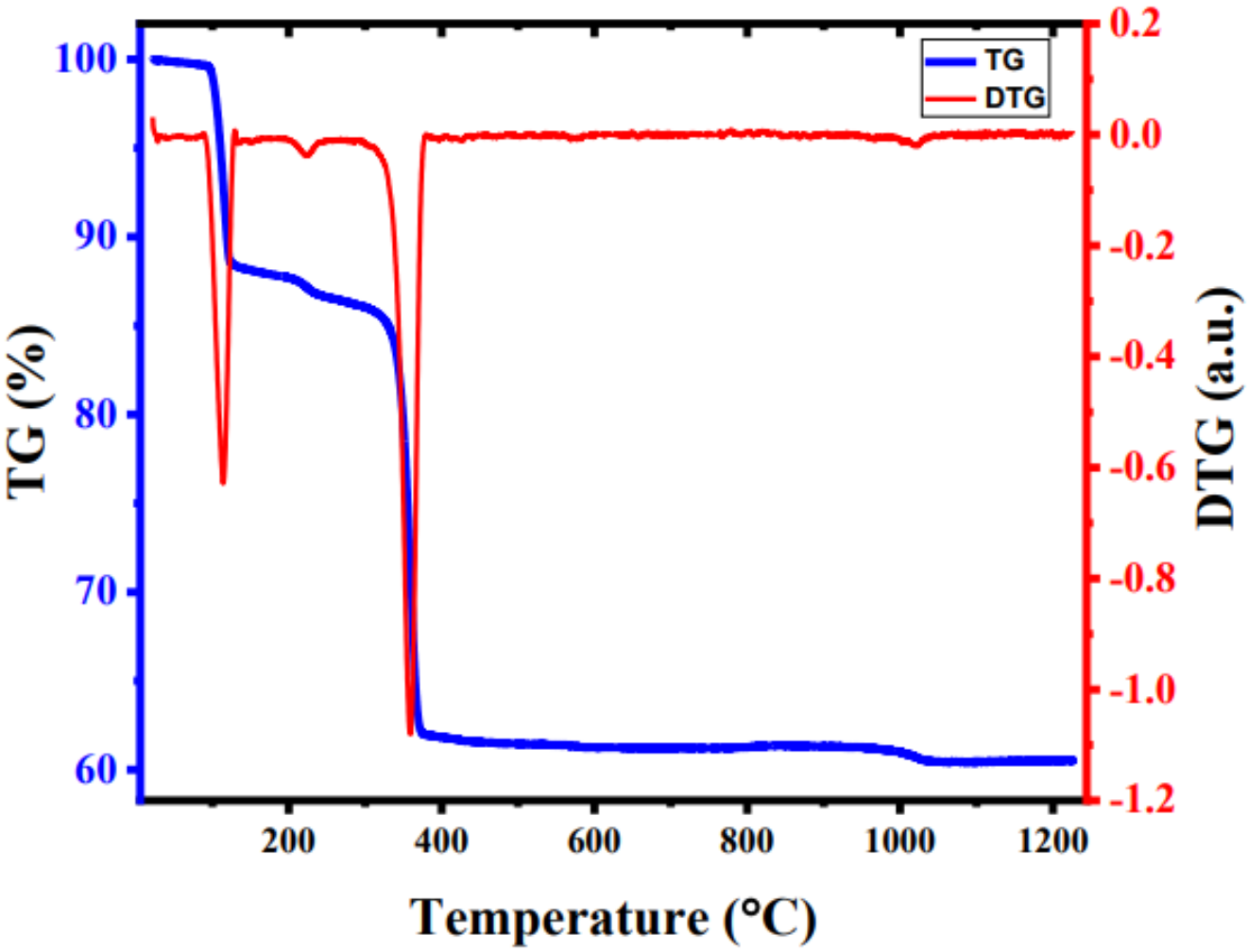

Fig. 1

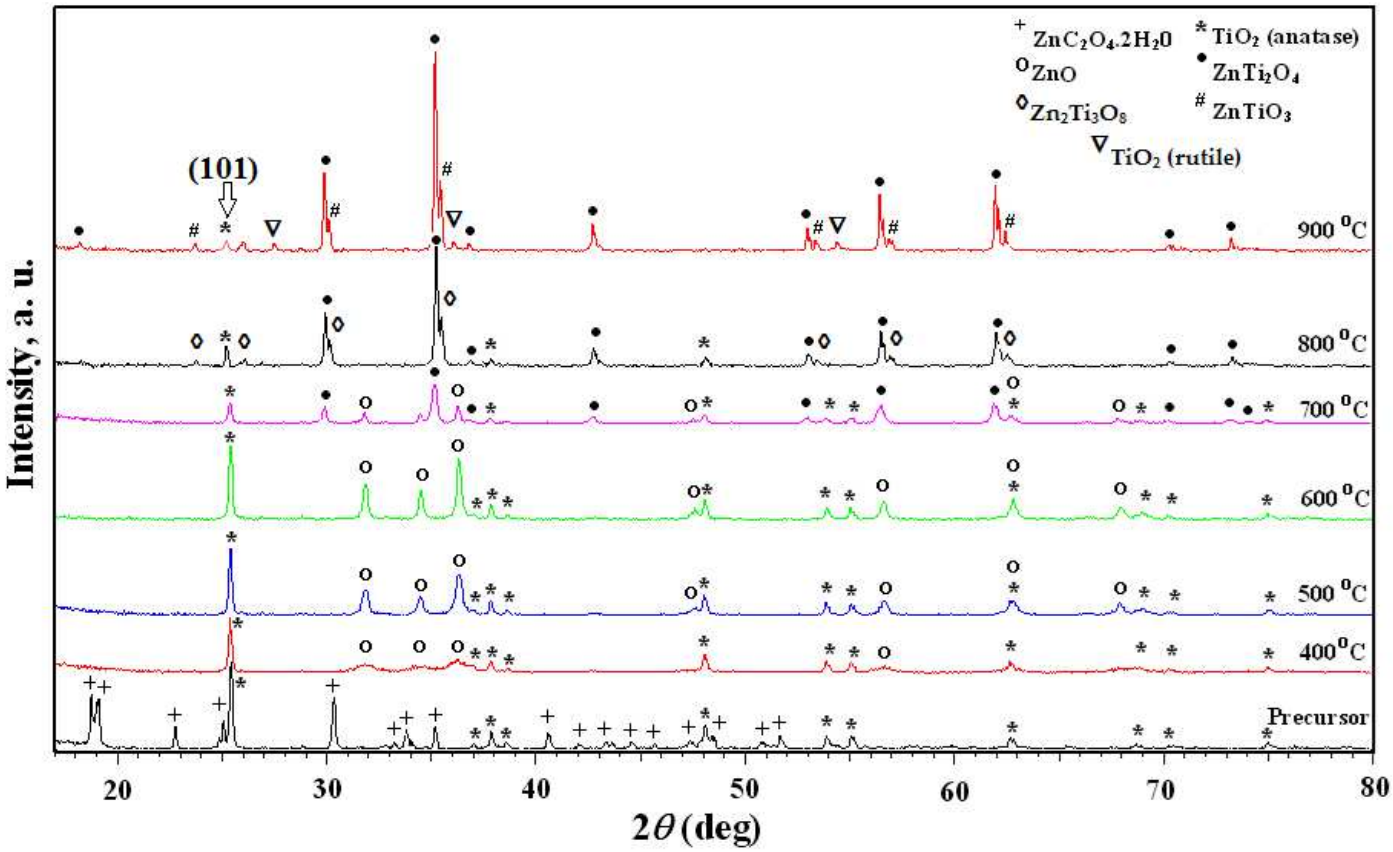
+ ZnC2O4.2H20
* TiO2 (anatase)
o ZnO
• ZnTi2O4
◊ Zn2Ti3O8
ZnTiO3
∇ TiO2 (rutile)
(101)
900 °C
800 °C
700 °C
600 °C
500 °C
400 °C
Precursor
Intensity, a. u.
2θ (deg)
20
30
40
50
60
70
80

Fig. 2

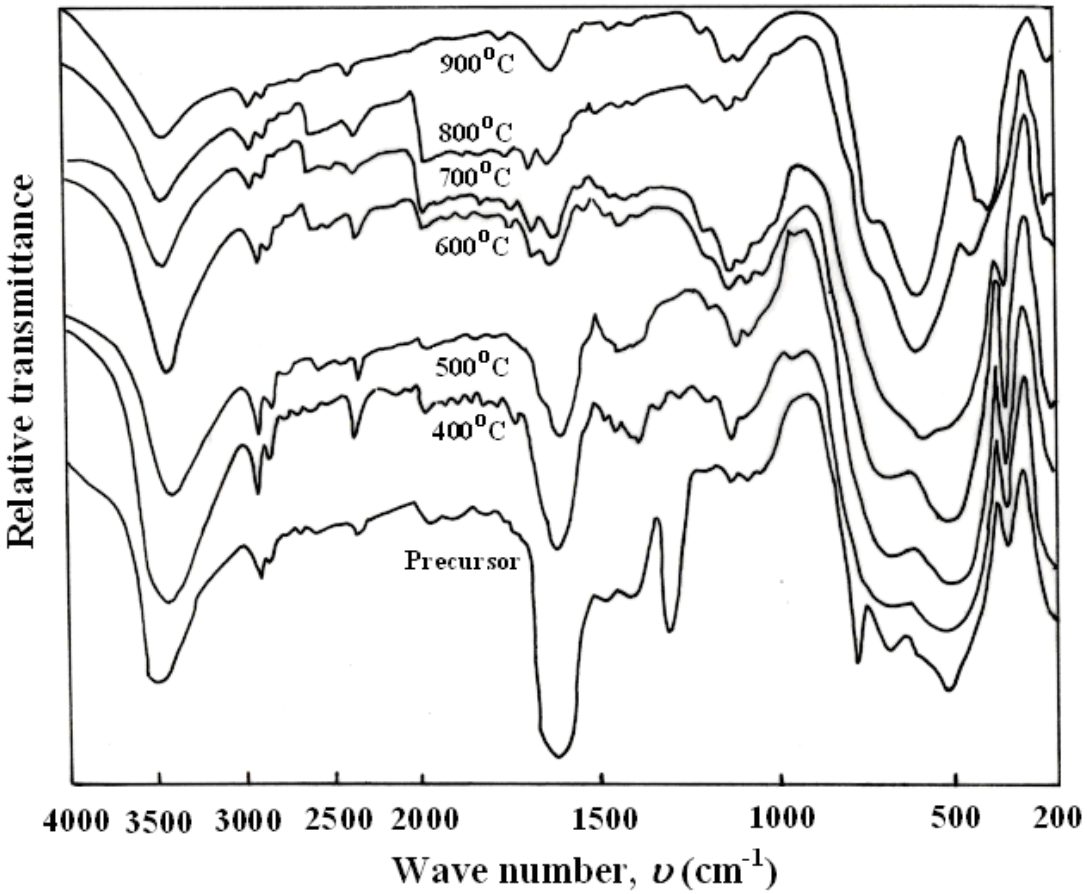
900°C
800°C
700°C
600°C
500°C
400°C
Precursor
Relative transmittance
4000 3500 3000 2500 2000 1500 1000 500 200
Wave number, υ (cm-1)

Fig. 3

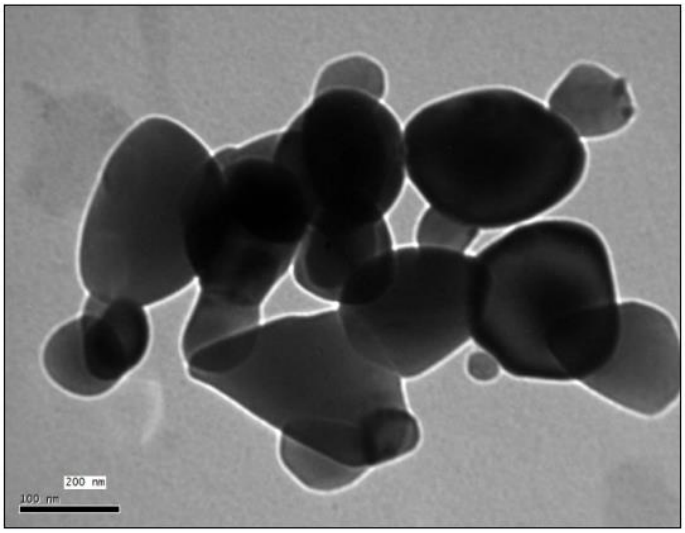
200 nm
100 nm

Fig. 4

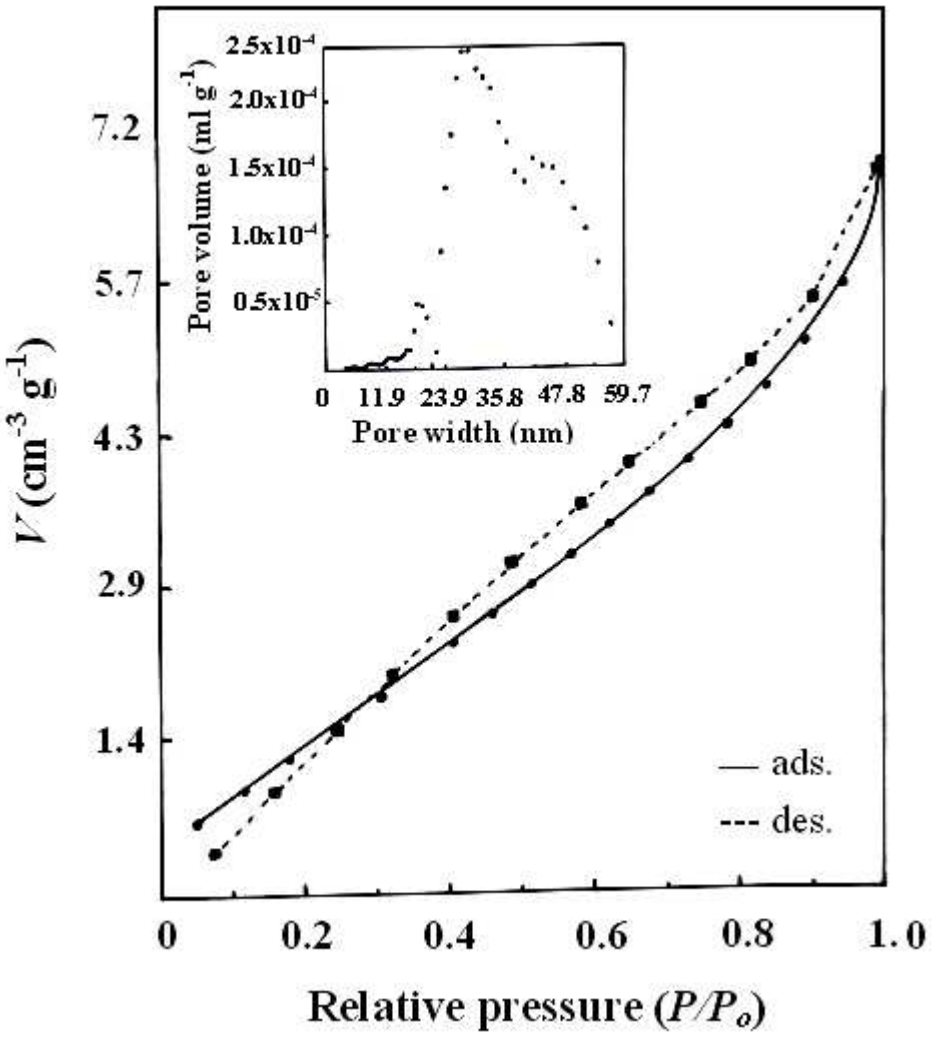
2.5x10⁻⁴
2.0x10⁻⁴
1.5x10⁻⁴
1.0x10⁻⁴
0.5x10⁻⁵
Pore volume (ml g⁻¹)
0 11.9 23.9 35.8 47.8 59.7
Pore width (nm)
7.2
5.7
4.3
2.9
1.4
V (cm⁻³ g⁻¹)
— ads.
--- des.
0 0.2 0.4 0.6 0.8 1.0
Relative pressure (P/Po)

Fig. 5

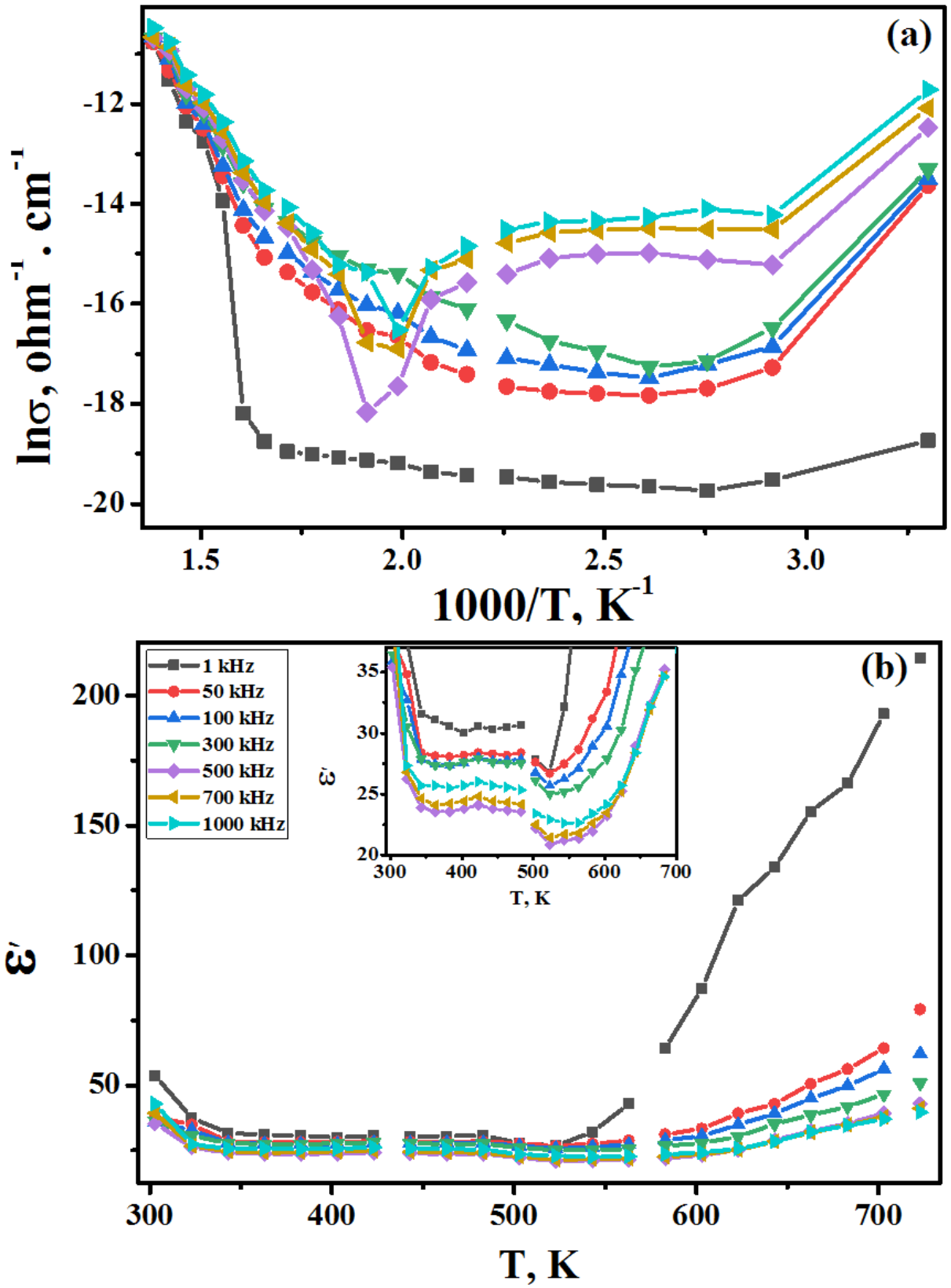
(a)
lnσ, ohm^{-1} . cm^{-1}
-12
-14
-16
-18
-20
1.5
2.0
2.5
3.0
1000/T, K^{-1}
(b)
ε'
200
150
100
50
300
400
500
600
700
T, K
1 kHz
50 kHz
100 kHz
300 kHz
500 kHz
700 kHz
1000 kHz
ε'
35
30
25
20
300
400
500
600
700
T, K

Fig. 6

Table 1. Activation energies calculated from ln σ vs. 1000/T plot as a function of frequencies for calcined precursor at 900°C for 2h

Frequency	E_a (eV)
1 kHz	2.52 ± 0.54
50 kHz	1.40 ± 0.07
100 kHz	1.34 ± 0.06
300 kHz	1.13 ± 0.05
500 kHz	1.11 ± 0.06
700 kHz	1.06 ± 0.07
1000 kHz	1.03 ± 0.05